ISSN 1070-3284, Russian Journal of Coordination Chemistry, 2014, Vol. 40, No. 6, pp. 432–438. © Pleiades Publishing, Ltd., 2014.

Synthesis, Crystal Structures, Antibacterial Activities, and Fluorescence Properties of Schiff Base Ligand and Its Nickel(II) Complex[1]

X. Zhang*, F. R. Li, C. Sun, M. Huang, and H. Zhang

Tianjin Key Laboratory of Structure and Performance for Functional Molecule, College of Chemistry, Tianjin Normal University, Tianjin, 300387 P.R. China

** e-mail: hxxyzx@mail.tjnu.edu.cn*

Received November 12, 2012

Abstract—A complex $[Ni(L \cdot CH_3OH)_2] \cdot CH_3OH$ was synthesized, in which a Schiff base ligand $HL \cdot CH_3OH$, was derived from condensation of 1-phenyl-3-methyl-4-(*p*-methylbenzoyl)-5-pyrazolone with L-Valine methyl ester. They were characterized by IR and single crystal X-ray diffraction. The ligand contains three independent molecules $L \cdot CH_3OH$. The complex has a dissociative methanol and nickel six-coordinated compound. Every fragment is a distorted octahedron with four oxygen atoms and two nitrogen atoms. The $HL \cdot CH_3OH$ ligand and its complex have been tested in vitro to evaluate their antibacterial activity against bacteria *Escherichia coli* and *Bacillus subtilis*. It has been found that the complex has higher activity than the corresponding free ligand $HL \cdot CH_3OH$ against the same bacteria. The $HL \cdot CH_3OH$ ligand and its complex have been tested by liquid fluorescent. It has been found that the complex has higher fluorescence property than ligand.

DOI: 10.1134/S1070328414060104

INTRODUCTION

During the past decades, lots of organic derivatives with Schiff base group have been extensively prepared and potentially applied as catalysis and enzymatic reactions, luminescent material, magnetism and molecular architectures [1–6]. Amino Acid Schiff base was an important biological ligand and has plenty of oxygen and nitrogen atoms. Besides, the metal complexes of amino acid Schiff base have catalytic aminotransferase and the racemate role, which can be used as an excellent model of studying vitamin B6 enzyme reaction [7] and O(2), N(2) carrier model compounds. The fluorescence properties [8], antibacterial, antiinflammatory, anticancer activity [9], can be used to determine metal ions and research chemotherapy drug [10–17]. In order to extend our knowledge of amino acid Schiff base complex chemistry, new L-valine methyl ester Schiff base ($HL \cdot CH_3OH$) and its Ni(II) complex $[Ni(L \cdot CH_3OH)_2] \cdot CH_3OH$ (**I**) have been synthesized and characterized by elemental analysis, IR, and single crystal X-ray diffraction. And their antibcterial activity against bacteria *Escherichia coli* and *Bacillus subtilis* were tested in vitro with agar diffusion method. For these complexes, the primary weak C–H···O hydrogen bond and C–H···π interactions afford 1D infinite linear architecture.

[1] The article is published in the original.

EXPERIMENTAL

Matetials and methods. Relovents used in the experiment: L-valine (biochemical reagent), perchloric acid nickle, anhydrous methanol, anhydrous ether were of analytical grade and used without further purification. IR spectra were recorded with a AVATAR_370 (Nicolet) spectrometer as KBr pellets between 4000–400 cm^{-1}. The elemental analyses (C, H, and N contents) were performed at CE-440 (Leeman-Labs) analyzer. ^1H NMR spectra of ligand were recorded with a Bruker 300MHz using $CDCl_3$ as solvent. Crystal structure was collected on a computer controlled by Bruker APEX II CCD diffractometer.

Synthesis of $HL \cdot CH_3OH$ ligand. Schiff base 1-phenyl-3-methyl-4-(*p*-methylbenzoyl)-5-pyrazoline ketone (HPMTP) was synthesized according to reference [18]. Using ethyl ether (80 mL) to solve L-valine methyl ester hydrochloride (10 mmol) and steaming out dry ammonia to neutralize the system accompanied with constant stirring. The L-valine methyl ester solution was obtained by filtrating, evaporating most of solvent and cooling (the yield was 60%); adding 10 mmol HPMTP of anhydrous ethanol solution (80 mL) and refluxing for 4–5 h. After the solvent was evaporated completely, recrystallization was carried on by mixed solvent of petroleum ether and ethyl acetate with volume ratio 4 : 1. Yellow powder was obtained and placed in a desiccator. Some compounds were dissolved in ethanol solution and yellow block-shaped crystals suitable for X-ray analysis were

obtained after one week. The yield of HL · CH_3OH was 65%.

For $C_{24}H_{26}N_3O_3$

anal. calcd. %:	C, 71.09;	H, 6.71;	N, 10.36.
Found, %:	C, 71.04;	H, 6.65;	N, 10.34.

IR (KBr; ν, cm^{-1}): 3444 ν(N–H), 1742 ν(C=O), 1627 ν(C=O) in pyrazoline cycle, 1542 δ(NH), 1156 ν(C–N). ^1H NMR ($CDCl_3$; δ, ppm): 1.48 (3H, CH_3), 2.45 (3H, CH_3), 0.97–1.06 (6H, $CH_3 \times 2$), 3.74 (3H, CH_3), 1.88 (1H, CH), 2.29 (1H, CH), 7.11–7.97 (9H, Ph–H), 11.59 (1H, NH).

Synthesis of complex I. Dropwised an anhydrous methanol solution (10 mL) of metal perchlorate (1 mol) to the solution of 2 mmol HL · CH_3OH in anhydrous methanol, used triethylamine to adjust to regulation pH 7.0, stirred for 1–2 h at room temperature, boiled under reflux on a water bath for 5–6 h. Then the resulting solution was filtered and left under the ambient environment for evaporation. After recrystallizing product with a mixture of petroleum ether and ethyl acetate (radio 10 : 1) and cooling, a certain yellow powder precipitated. After filtration, use ethanol to wash the power 2–3 times in the dry desiccator. Some compounds were dissolved in ethanol solution and green blocked shaped crystals suitable for X-ray analysis were obtained within a few days. The yield of **I** was 72%.

For $C_{49}H_{54}N_6O_7Ni$

anal. calcd., %:	C, 66.43;	H, 6.03;	N, 9.65.
Found, %:	C, 66.45;	H, 6.04;	N, 9.69.

IR (KBr; ν, cm^{-1}): 1527 ν(C=N), 1684 ν(C=O), 1602 ν(C=O) in pyrazoline cycle.

X-ray crystallography. Select a partion of single crystals (0.28 × 0.22 × 0.20 mm) of ligand and complex **I** for X-ray diffraction experiments. A Bruker APEX II CCD diffractometer with a CCD area detector was employed for data collection using monochromatic MoK_α radiation (λ = 0.71073 Å) monochromated by graphite. Using a θ–ω scan technique at 296(2) K, the structures were solved by direct methods and refined with the full matrix least-squares technique using the SHELXS-97 and SHELXL-97 programs [19, 20]. The crystallographic data and selected bond lengths and angles are listed in Tables 1 and 2, respectively.

Determination of antibacterial activities. The antibacterial acitivities against Gram negative *Escherichia coli*, Gram positive *Bacillus subtilis* of Schiff base and its transition metal complex were measured by agar diffusion method [21]. Beef extract protein agar culture medium, experimental containers and oxford cup were placed in an autoclave and sterilized for 20 min after the pressure was up to 1.1 kg. After being activated for third times, strains were vaccinated to the culture medium and kept in the incubator at the temperature of 37 ± 1°C for 16 h. The culture medium which was melted and cooled to 50°C was poured into the culture dish and paved equably in the sterilization room. When the culture medium of agar become solidified, the 0.20 mL liquid of germ with the concentration of 10^8 colony forming units per mL was putted into culture dish and paved with flexural glass rod. The sterilized oxford cup was burned on the sprit lamp and pasted to the culture dish. The 0.20 mL drug liquid with different consistency which were resolved with *N*,*N*-dimethylformamide (DMF) was injected to the oxford cup. These plates were incubated around the clock at 37 ± 1°C. After that, the diameter of the inbition ring was determined.

RESULT AND DISCUSSION

The crystal structures of ligand and complex **I** are shown in Figs. 1 and 2. Taking into account the measurement error and all component atoms are light atoms such as C, H, O, N, the anomalous scattering factor in the conclusion are small, so in this case that the Flack factor of –0.2 leads to the judgmehent of absolute configuration is of highly credibility. The HL · CH_3OH ligand is characterized by the presence of three independent subunits (**I**, **II**, **III**) and into a large conjugated system, not only leads to the redistribution of charge, but also contributes to the migration of the proton, which causes such condensation reaction not to form the imine structure, but through proton migration to form enamine ketone structure.

In this compound, both bond lengths of C(8)–C(11), C(32)–C(35), C(56)–C(59) (1.396, 1.393 1.362 Å) are between the figure of C–C and C=C, bond lengths of C(11)–N(3), C(35)–N(6), C(59)–N(9) (1.329, 1.337, 1.340 Å) are between the figure of C–N and C=N. Meanwhile, the bond length of C(7)–O(1), C(31)–O(4), C(55) –O(7) (1.252, 1.243, 1.250 Å) is a typical C=O bond length, therefore these three independent subunits in the ligand are enamino ketone structure, rather than the ideal Schiff base (–C=N–) structure [22, 23]. Bond lengths of subunits **I**, **II**, **III** in five-member pyrazole cycles are between the single and double bond length. In the compound, C(5), C(25) and C(49) act as donors to form intramolecular hydrogen bonds C(5)–H(5)···O(1), C(25)–H(25)···O(4), C(49)–H(49)···O(7) with oxygen atoms (O(1), O(4), O(7), which are helpful to consolidate the structure. It also indicates the compound is enamino ketone structure and occupied with six-member chelate rings in order to reduce system energy.

In the asymmetric unit of complex **I** one crystallographic independent nikel(II) center was six-coordinated with two nitrogen atoms N(3), N(6) from different L-ligands in axial directions, two carbonyl oxygen atoms O(2), O(5) from chelate cycle and two oxygen

Table 1. Crystallographic data and structure refinement for ligand and complex **I**

Parameter	Value	
	$HL \cdot CH_3OH$	**I**
Empirical formula	$C_{24}H_{26}N_3O_3$	$C_{49}H_{54}N_6O_7Ni$
Formula weight	404.48	898.70
Crystal size, mm	0.28 × 0.22 × 0.20	0.28 × 0.22 × 0.20
Crystal system	Orthorhombic	Monoclinic
Space group	$P2_12_12_1$	$P2_1$
a, Å	9.9057(6)	10.367(2)
b, Å	17.7063(10)	18.156(4)
c, Å	38.839(2)	12.486(3)
β, deg	90	99.865(4)
V, Å^3	6812.1(7)	2315.6(9)
Z	12	2
ρ_{calcd}, g cm^{-3}	1.183	1.289
μ, mm^{-1}	0.079	0.476
F(000)	2580	950
Reflections collected	35285	11653
Independent reflections (R_{int})	12012 (0.0627)	6267 (0.0436)
Refinement parameters	827	577
Goodness-of-fit	0.975	1.093
R_1 ($I > 2\sigma(I)$)	0.0517	0.0687
wR_2* (all data)	0.1214	0.1676

* Final weighting scheme: $w = 1/[\sigma^2(F_o^2) + (0.0898P)^2 + 0.1127P]$, $P = (F_o^2 + 2F_c^2)/3'$ for ligand; $w = 1/[\sigma^2(F_o^2) + (0.0348P)2 + 0.1165P]$, $P = (F_o^2 + 2F_c^2)/3'$ for complex.

atoms O(1), O(4) from L-valine methyl ester in the equatorial plane forming two five-membered chelate rings and two six-membered chelate rings. And besides, O(1), O(4) have shorter bond lengths with Ni, when compared with that of O(2), O(5) and N(3), N(6), and Ni, illuminating the correspondination to the stronger coordination ability.The bond distances of Ni–O and Ni–N range from 1.971(6) to 2.151(6) Å, which means that ligand coordinated with Ni(1) in a distorted octahedral coordination geometry (Fig. 2).

As show in Fig. 2, in the complex molecules, there are two distinct intermolecular hydrogen bonds C(37)–H(37)···O(7), C(44)–H(44)···O(7) which contribute to the 1D zigzag tape, and through the inter-C(13)–H(13)···π weak interactions, different conformations of complex molecules and dissociative methanol molecules linked into the unlimited extension of the one-dimensional supramolecular structure chain (Fig. 3). Hydrogen bond geometries of the complex are listed in Table 3.

As shown in Table 4, both $HL \cdot CH_3OH$ molecule and complex **I** can certainly inhibit growth of bacteria *E. coli* and *Bacillus subtilis*. And the activity is stronger at *Escherichia coli*. Both ligand and complex **I** have higher antibacterial activity for bacteria *E. coli* than HPMTP, and ligand generally acts more active, which is related to the biological function of nickle element. Such phenomenon is analogous to the Schiff base complex derived from HPMTP and furfuryl amine. The diversification with concentration of inhibitory effect did not present a linear relationship, but reach a peak at a certain concentration.

The fluorescence spectra of $HL \cdot CH_3OH$ ligand and complex **I** were determined at room temperature in methanol–water solution. Excitating the microc-

Table 2. Select bond lengths (Å) and bond angles (deg) for ligand and complex **I**

Bond	*d*, Å	Bond	*d*, Å	Bond	*d*, Å
Molecule HL · CH_3OH					
O(1)–C(9)	1.252(5)	O(4)–C(31)	1.243(5)	O(7)–C(55)	1.250(6)
O(2)–C(23)	1.191(6)	O(5)–C(47)	1.188(5)	O(8)–C(71)	1.192(6)
O(3)–C(23)	1.328(5)	O(6)–C(47)	1.314(5)	O(9)–C(71)	1.298(6)
O(3)–C(24)	1.444(6)	O(6)–C(48)	1.468(6)	O(9)–C(72)	1.439(7)
N(1)–C(9)	1.379(6)	N(4)–C(31)	1.378(5)	N(7)–C(55)	1.359(6)
N(1)–N(2)	1.391(5)	N(4)–N(5)	1.403(5)	N(7)–N(8)	1.385(5)
N(1)–C(6)	1.430(5)	N(4)–C(30)	1.410(5)	N(7)–C(54)	1.413(6)
N(2)–C(7)	1.311(5)	N(5)–C(33)	1.313(5)	N(8)–C(57)	1.311(5)
N(3)–C(11)	1.329(5)	N(6)–C(35)	1.337(5)	N(9)–C(59)	1.340(6)
N(3)–C(19)	1.450(5)	N(6)–C(43)	1.466(5)	N(9)–C(67)	1.485(6)
C(7)–C(8)	1.424(6)	C(32)–C(33)	1.418(5)	C(56)–C(57)	1.407(7)
C(7)–C(10)	1.483(6)	C(33)–C(34)	1.503(6)	C(57)–C(58)	1.490(7)
C(8)–C(11)	1.396(6)	C(32)–C(35)	1.393(5)	C(56)–C(59)	1.362(6)
C(8)–C(9)	1.428(6)	C(31)–C(32)	1.446(6)	C(55)–C(56)	1.434(7)
C(19)–C(23)	1.492(7)	C(43)–C(47)	1.487(7)	C(67)–C(71)	1.480(8)
C(19)–C(20)	1.558(7)	C(43)–C(44)	1.536(6)	C(67)–C(68)	1.551(8)
Complex **I**					
Ni(1)–O(1)	1.971(6)	O(3)–C(24)	1.461(13)	N(3)–C(11)	1.291(9)
Ni(1)–O(4)	1.998(5)	O(4)–C(31)	1.269(9)	N(3)–C(19)	1.509(10)
Ni(1)–N(3)	2.046(6)	O(5)–C(47)	1.223(9)	N(4)–C(31)	1.349(10)
Ni(1)–N(6)	2.060(6)	O(6)–C(47)	1.288(9)	N(4)–N(5)	1.404(9)
Ni(1)–O(2)	2.130(6)	O(6)–C(48)	1.478(12)	N(4)–C(30)	1.429(9)
Ni(1)–O(5)	2.151(6)	N(1)–C(7)	1.376(10)	N(5)–C(33)	1.290(10)
O(1)–C(7)	1.270(8)	N(1)–C(6)	1.392(11)	N(6)–C(35)	1.294(10)
O(2)–C(23)	1.200(10)	N(1)–N(2)	1.394(9)	N(6)–C(43)	1.481(10)
O(3)–C(23)	1.284(11)	N(2)–C(9)	1.349(11)	C(49)–O(7)	1.411(16)
Angle	ω, deg	Angle	ω, deg	Angle	ω, deg
Molecule HL · CH_3OH					
C(23)O(3)C(24)	118.3(4)	C(47)O(6)C(48)	116.5(4)	C(71)O(9)C(72)	118.4(5)
C(9)N(1)N(2)	112.3(4)	C(31)N(4)N(5)	111.1(3)	C(55)N(7)N(8)	112.3(4)
C(9)N(1)C(6)	128.7(4)	C(31)N(4)C(30)	130.3(4)	C(55)N(7)C(54)	129.0(5)
N(2)N(1)C(6)	118.7(4)	N(5)N(4)C(30)	118.3(4)	N(8)N(7)C(54)	118.6(4)
C(7)N(2)N(1)	106.1(4)	C(33)N(5)N(4)	106.6(3)	C(57)N(8)N(7)	106.1(4)
C(11)N(3)C(19)	125.3(4)	C(35)N(6)C(43)	124.2(4)	C(59)N(9)C(67)	126.2(4)
N(2)C(7)C(8)	111.3(4)	N(5)C(33)C(32)	112.0(4)	N(8)C(57)C(56)	111.4(4)
N(2)C(7)C(10)	118.3(4)	N(5)C(33)C(34)	119.2(4)	N(8)C(57)C(58)	118.3(5)
C(11)C(8)C(7)	132.1(4)	C(35)C(32)C(33)	132.0(4)	C(59)C(56)C(57)	131.7(5)
C(11)C(8)C(9)	121.9(4)	C(35)C(32)C(31)	122.6(4)	C(59)C(56)C(55)	122.6(5)
C(7)C(8)C(9)	106.0(4)	C(33)C(32)C(31)	105.2(4)	C(57)C(56)C(55)	105.7(4)
O(1)C(9)N(1)	126.1(4)	O(4)C(31)N(4)	125.5(4)	O(7)C(55)N(7)	126.0(5)
N(1)C(9)C(8)	104.2(4)	N(4)C(31)C(32)	105.2(4)	N(7)C(55)C(56)	104.5(5)
N(3)C(11)C(8)	118.0(4)	N(6)C(35)C(32)	118.9(4)	N(9)C(59)C(56)	118.7(4)
N(3)C(11)C(12)	121.2(4)	N(6)C(35)C(36)	119.8(4)	N(9)C(59)C(60)	119.6(4)
N(3)C(19)C(23)	108.7(4)	N(6)C(43)C(47)	107.6(4)	N(9)C(67)C(68)	111.2(5)
N(3)C(19)C(20)	108.6(4)	N(6)C(43)C(44)	111.3(4)	N(9)C(67)H(67)	108.3
O(2)C(23)O(3)	123.2(5)	O(5)C(47)O(6)	123.3(5)	O(8)C(71)O(9)	123.9(7)
Complex **I**					
O(1)Ni(1)O(4)	90.1(2)	N(6)Ni(1)O(2)	95.7(2)	C(31)O(4)Ni(1)	117.6(5)
O(1)Ni(1)N(3)	93.0(2)	O(1)Ni(1)O(5)	87.5(2)	C(47)O(5)Ni(1)	112.2(5)
O(4)Ni(1)N(3)	90.2(2)	O(4)Ni(1)O(5)	172.0(2)	C(47)O(6)C(48)	116.8(7)
O(1)Ni(1)N(6)	91.6(2)	N(3)Ni(1)O(5)	97.6(2)	C(11)N(3)Ni(1)	125.2(5)
O(4)Ni(1)N(6)	93.6(2)	N(6)Ni(1)O(5)	78.8(2)	C(19)N(3)Ni(1)	114.2(4)
N(3)Ni(1)N(6)	174.0(3)	O(2)Ni(1)O(5)	92.6(2)	C(35)N(6)Ni(1)	125.2(5)
O(1)Ni(1)O(2)	172.6(2)	C(7)O(1)Ni(1)	118.1(5)	C(43)N(6)Ni(1)	114.1(5)
O(4)Ni(1)O(2)	90.8(2)	C(23)O(2)Ni(1)	112.6(6)	O(4)C(31)N(4)	122.0(7)
N(3)Ni(1)O(2)	79.7(2)	C(23)O(3)C(24)	114.9(9)	O(2)C(23)C(19)	124.9(9)

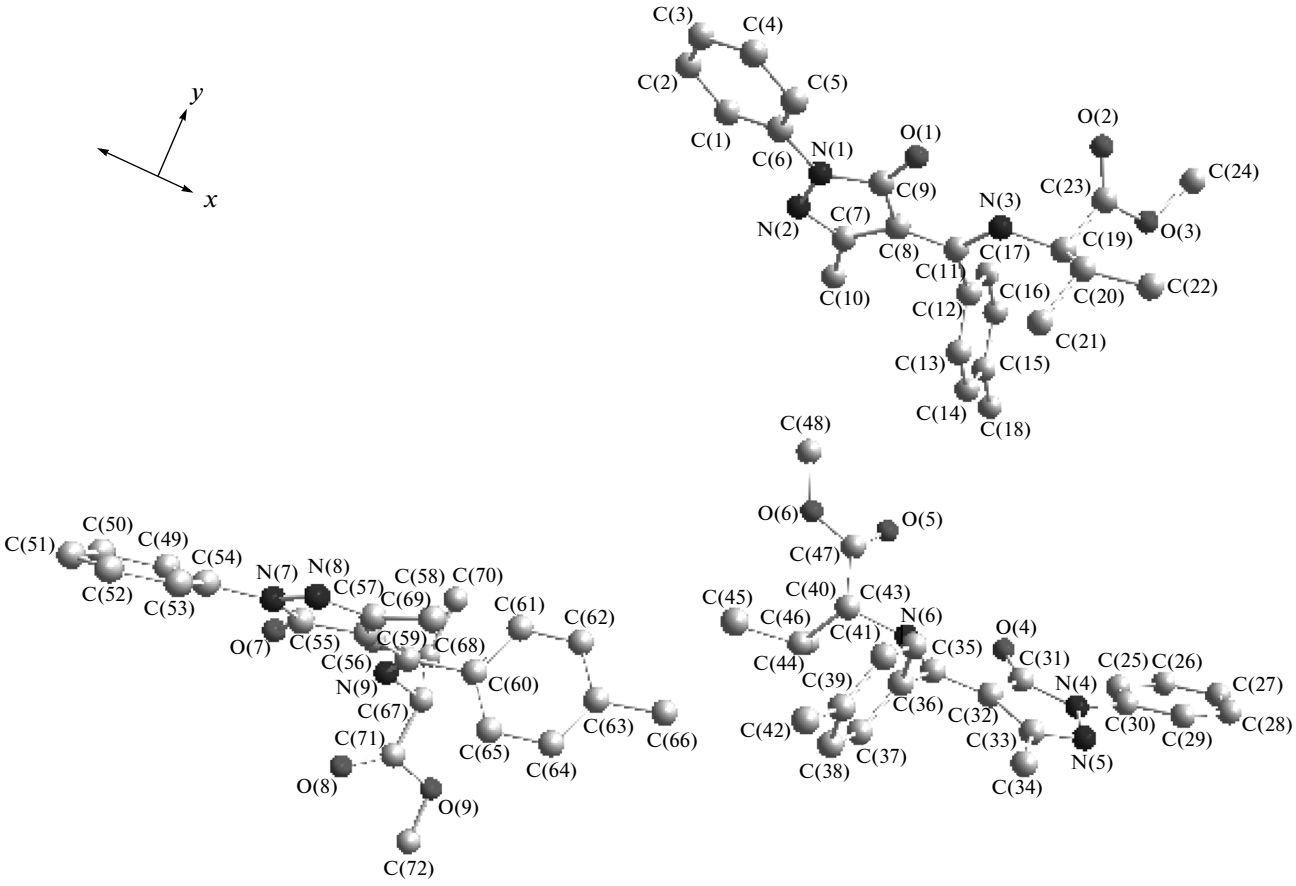

Fig. 1. Three independent molecules in crystal HL · CH_3OH.

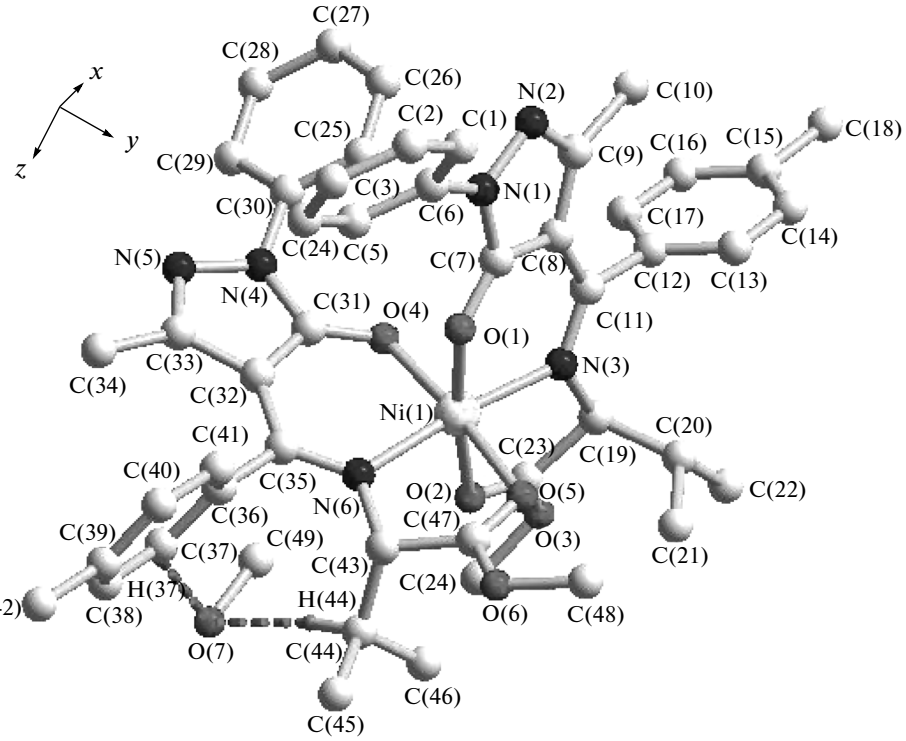

Fig. 2. The local coordination environment of the Ni(II) atom of complex **I** (H atoms were omitted for clarity).

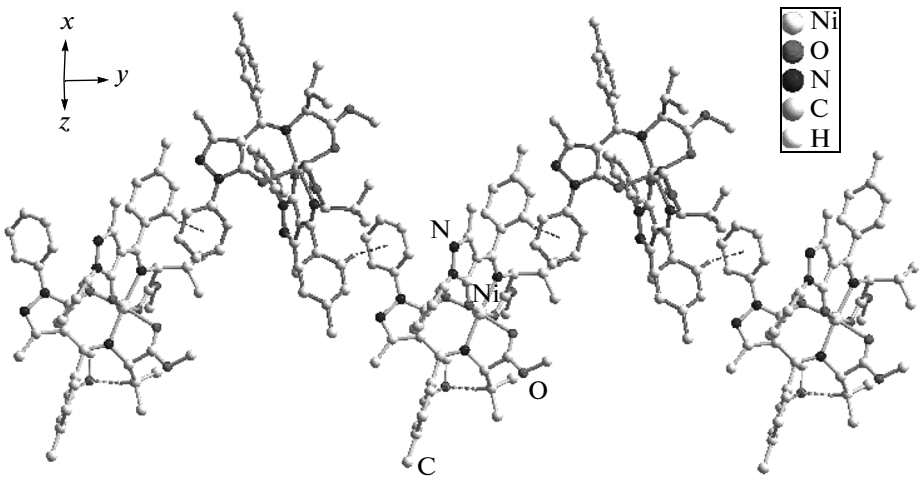

Fig. 3. 1D Molecular structure of complex **I**.

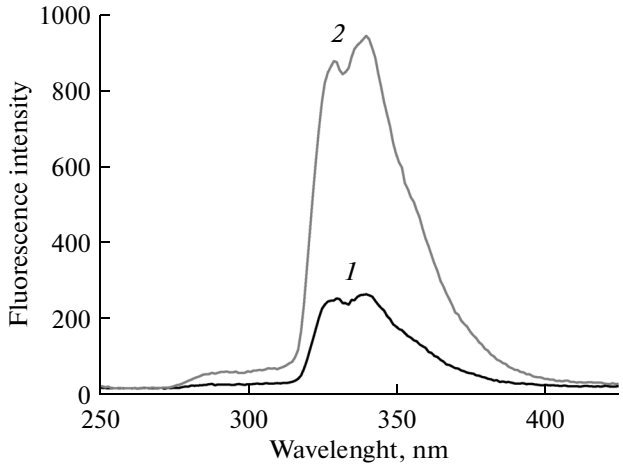

Fig. 4. Fluorescent emission spectra of ligand (*1*) and complex (*2*) **I**.

rystalline ligand sample at 238 nm produces intense emission with peak maximum at 340 nm (Fig. 4). The emission spectrum of complex is similar to that of HL · CH_3OH with difference in the emission intensity, displaying emission peak at 340 nm. Thus, we can presume that the emission of ligand should originate from the $\pi \rightarrow \pi^*$ transitions in the ligand. Both complex and rigid ligand have fine conjugated system, but because

Table 3. Structural parameters of hydrogen bonds for complex **I**

D–H···A	Distance, Å			Angle DHA, deg
	D–H	H···A	D···A	
O(7)–H(7)···N(2)	0.82	2.00	2.79	160
C(37)–H(37)···O(7)	0.93	2.34	3.22	156
C(44)–H(44)···O(7)	0.98	2.60	3.54	162
C–H···Cg(*I*)	H–Cg(*I*)	H–Perp(*I*)	X–H···Cg(*I*)	X–Cg(*I*)
C(13)–H(13)···Cg(9)	0.93	2.57	3.50	173

Table 4. Antibacterial activity data of ligand and complex **I**

Compound	Concentration, g/L	Bacterial species, mm	
		Escherichia coli	*Bacillus subtilis*
HPMTP	5.0	32.5	28.8
	2.5	44.6	41.3
	1.25	36.1	32.5
Ligand	5.0	63.9	57.5
	2.5	48.2	45.0
	1.25	63.9	41.3
Complex **I**	5.0	84.3	82.5
	2.5	51.8	50.0
	1.35	92.8	91.3

of the nickle ion in the complex, it can effectively transport energy from activated form to nickle ion. So the complex can be potentially used as fluorescence material.

REFERENCES

1. Li, J., Li, Z., and Liu, L., *Inorg. Chim. Acta*, 2007, vol. 360, p. 1995.
2. Brana, M.F., Gradillas, A., and Ovalles, A.G., *Bioorg. Med. Chem.*, 2006, vol. 14, p. 9.
3. Zhang, G.L., Dai, B.Q., and Li, J.Z., *J. Inorg. Chem.*, 2003, vol. 19, p. 1331.
4. Luo, Z.M., Yu, Q., and Yang, C., *Chem. Reagents*, 2003, vol. 25, p. 193.
5. Yu, Z.G., Li, J.Z., and Liu, S.Q., *Appl. Chem.*, 2004, vol. 21, p. 1300.
6. Habibi, M.H., Mokhtari, R., Harrington, R.W., and Clegg, W., *Acta Crystallogr., Sect. E: Structure Reports Online*, 2007, vol. 63, p. 2881.
7. Li, D.Q. and Zhou, S., *J. Guangxi Sci.*, 2009, vol. 16, p. 73.
8. Aoki, I., Takahashi, A., and Watanabek, K., *Bull. Chem. Soc. Jpn.*, 1990, vol. 63, p. 1973.
9. Dutta, R.L. and Das, B.R., *J. Sci. Ind. Res.*, 1988, vol. 47, p. 41.
10. Wang, C.G., Zhu, X.D., and Zhang, C.C., *J. Huazhong Normal Univ.*, 1995, vol. 29, p. 336.
11. Yang, Z.Y., Ai, J., and Wang, L.F., *J. Lanzhou Univ.*, 1993, vol. 29, p. 1620.
12. Patrick, D. and Prasad, P., *Inorg. Chem.*, 2003, vol. 42, p. 7366.
13. Feng, X.Z., Xia, J.H., and Liu, Z., *Chem. Res. Appl.*, 2007, vol. 19, p. 1155.
14. Li, J.P., Ji, Y., and Liu, R.J., *Chem. Res. Appl.*, 2008, vol. 20, p. 87.
15. Casella, L. and Gullotti, M., *Inorg. Chem.*, 1986, vol. 25, p. 1293.
16. Guzow, K. and Milewska, M., *Tetrahedron*, 2004, vol. 60, p. 11889.
17. Tshuva, E.Y. and Lippard, S.J., *Chem. Rev.*, 2004, vol. 104, p. 987.
18. Huang, M., *Thesis for the Master of Tianjing Normal Univ.*, 2010.
19. Sheldrick, G.M., *SHELXL-97, Program for X-ray Crystal Structure Refinement*, Göttingen (Germany): Univ. of Göttingen, 1997.
20. Sheldrick, G.M., *SHELXL-97, Program for X-ray Crystal Structure Solution*, Göttingen (Germany): Univ. of Göttingen, 1997.
21. Wang, J.L., Zhang X., Yu M., et al., *Polish J. Chem.*, 2001, vol. 75, p. 1367.
22. Yuan, Z.L., Hu, Q.H., and Wu, Q., *Appl. Chem. Industry*, 2008, vol. 37, p. 196.
23. Jing, L.X., Liu, Z., and Xia, J.H., *Metallurgical Analysis*, 2008, vol. 28, p. 14.